

Contribution from the Departments of Chemistry, State University of New York at Buffalo, Buffalo, New York 14214, and The Ohio State University, Columbus, Ohio 43210

## Structural Studies on Polynuclear Osmium Carbonyl Hydrides. 22.<sup>1</sup> Crystal Structure and <sup>13</sup>C NMR Spectra of $(\mu\text{-H})_2\text{Os}_3\text{Fe}(\text{CO})_{13}$

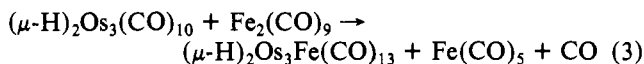
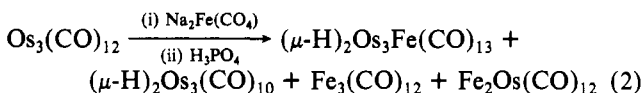
MELVYN ROWEN CHURCHILL,<sup>\*2</sup> CLIFFORD BUENO,<sup>2</sup> WEN LIANG HSU,<sup>3</sup> JEFFREY S. PLOTKIN,<sup>3</sup> and SHELDON G. SHORE<sup>\*3</sup>

Received October 20, 1981

The heteronuclear metal cluster compound  $(\mu\text{-H})_2\text{Os}_3\text{Fe}(\text{CO})_{13}$ , prepared from  $(\mu\text{-H})_2\text{Os}_3(\text{CO})_{10}$  and  $\text{Fe}_2(\text{CO})_9$ , has been examined via variable-temperature <sup>13</sup>C NMR spectroscopy and a single-crystal X-ray diffraction study. This complex crystallizes in the centrosymmetric monoclinic space group *C2/c* (No. 15) with  $a = 31.444$  (6) Å,  $b = 9.700$  (1) Å,  $c = 13.935$  (3) Å,  $\beta = 110.99$  (1)°,  $V = 3968.0$  Å<sup>3</sup>, and  $\rho(\text{calcd}) = 3.32$  g cm<sup>-3</sup> for  $Z = 8$  and mol wt 992.60. Diffraction data were collected with a Syntex P2<sub>1</sub> automated four-circle diffractometer, and the structure was refined to  $R_F = 5.7\%$  and  $R_{wF} = 6.2\%$  for all 2598 reflections with  $3.5^\circ < 2\theta < 45.0^\circ$  (Mo K $\alpha$  radiation). All atoms were located and refined in the course of the analysis. The molecule contains a tetrahedral Os<sub>3</sub>Fe core and has approximate *C<sub>s</sub>* symmetry. Each osmium atom is linked to three terminal carbonyl ligands, while the iron atom is bound to four carbonyl ligands, two of which are strictly terminal and two of which are of the "semibridging" type [Fe-C(11) = 1.823 (22) Å, Os(1)---C(11) = 2.341 (20) Å,  $\angle\text{Fe-C(11)-O(11)} = 152.5$  (18)°; Fe-C(12) = 1.854 (22) Å, Os(3)---C(12) = 2.346 (21) Å,  $\angle\text{Fe-C(12)-O(12)} = 153.6$  (18)°]. The semibridged Os-Fe bonds [Os(1)-Fe = 2.686 (3) Å, Os(3)-Fe = 2.686 (3) Å] are slightly shorter than the nonbridged Os(2)-Fe bond of 2.717 (2) Å, and the hydrido-bridged Os-Os bonds [Os(1)-Os(2) = 2.934 (1) Å, Os(2)-Os(3) = 2.937 (1) Å] are substantially longer than the nonbridged Os(1)-Os(3) bond of 2.847 (1) Å. The bridging hydride ligands were located directly in the analysis; their disposition about the tetrahedral edges is discussed in detail.

### Introduction

The complex  $(\mu\text{-H})_2\text{Os}_3\text{Fe}(\text{CO})_{13}$  has previously been synthesized in low yield (7%) by Moss and Graham<sup>4</sup> as shown in eq 1 and in  $\leq 9\%$  yield by Geoffroy and Gladfelter<sup>5</sup> as shown in eq 2. We now report a high-yield ( $\sim 82\%$ ) synthesis of  $(\mu\text{-H})_2\text{Os}_3\text{Fe}(\text{CO})_{13}$  from  $(\mu\text{-H})_2\text{Os}_3(\text{CO})_{10}$  (see eq 3), along with a single-crystal X-ray diffraction study and variable-temperature <sup>13</sup>C NMR spectra of this heteronuclear complex. A preliminary account of the synthetic route has appeared previously.<sup>6</sup>



### Experimental Section

**Preparation of  $(\mu\text{-H})_2\text{Os}_3\text{Fe}(\text{CO})_{13}$ .** About 20 mL of benzene was condensed into a two-necked 50-mL flask containing  $(\mu\text{-H})_2\text{Os}_3(\text{CO})_{10}$  (0.3 g, 0.35 mmol) and  $\text{Fe}_2(\text{CO})_9$  (0.26 g, 0.70 mmol). The mixture was then warmed to room temperature and stirred at this temperature for 20 h. The benzene was then removed from the reaction mixture with use of a rotary evaporator under reduced pressure to leave a brownish red solid, which was washed with 10 mL of a 1:1 benzene/hexane mixture. The remaining undissolved solid was  $(\mu\text{-H})_2\text{Os}_3\text{Fe}(\text{CO})_{13}$  and was purified by recrystallization from  $\text{CH}_2\text{Cl}_2$ /hexane at  $-10^\circ\text{C}$  to afford 0.26 g of finely divided orange-red crystals. The benzene/hexane washings were chromatographed on a preparative TLC plate (silica gel) with a 1:4 benzene/hexane solvent

Table I. Data for X-ray Study of  $(\mu\text{-H})_2\text{Os}_3\text{Fe}(\text{CO})_{13}$

(A) Crystal Parameters at 23 °C	
cryst syst: monoclinic	$V = 3968.0$ Å <sup>3</sup>
space group: <i>C2/c</i> (No. 15)	$Z = 8$
$a = 31.444$ (6) Å	mol wt = 992.60
$b = 9.700$ (1) Å	$\rho(\text{calcd}) = 3.32$ g cm <sup>-3</sup>
$c = 13.935$ (3) Å	$\mu = 210.9$ cm <sup>-1</sup>
$\beta = 110.99$ (1)°	
(B) Data Collection	
diffractometer: Syntex P2 <sub>1</sub>	
radiation: Mo K $\alpha$ ( $\lambda = 0.710730$ Å)	
monochromator: highly oriented graphite, equatorial mode	
reflectns measd: $\pm h, \pm k, +l$ for $2\theta = 3.5\text{--}45.0^\circ$	
scan type: $\omega$ scan over $1.0^\circ$ at $1.5^\circ \text{ min}^{-1}$ ( $0.8^\circ$ offset for bkgds)	
reflectns collected: 3008 total, merged to 2598 independent reflectns	
std reflectns: 3 measd after each 97 reflectns ( $\overline{22}, 0, 0; 060; 008$ ); no decay obsd	

mixture as eluent. A 0.018-g fraction of  $(\mu\text{-H})_2\text{Os}_3\text{Fe}(\text{CO})_{13}$  was obtained to give a combined yield of 0.28 g. Infrared and <sup>1</sup>H NMR spectra were in good agreement with those reported previously.<sup>5,6</sup> A <sup>13</sup>C-enriched sample for NMR studies was prepared in the same manner except that 25% <sup>13</sup>C-enriched  $(\mu\text{-H})_2\text{Os}_3(\text{CO})_{10}$  was employed.

Crystals of  $(\mu\text{-H})_2\text{Os}_3\text{Fe}(\text{CO})_{13}$  were obtained by slow recrystallization from  $\text{CH}_2\text{Cl}_2$ /hexane at  $-10^\circ\text{C}$ .

**Collection of <sup>13</sup>C NMR Spectra.** Carbon-13 NMR spectra were obtained on a Bruker HX-90 FT spectrometer operating at 22.62 MHz. Chemical shifts are reported relative to  $\text{Me}_4\text{Si}$  (0.0 ppm). Proton-coupled and -decoupled spectra were recorded in a mixture of 75% THF (normal isotopic composition) and 25%  $\text{CDCl}_3$  at  $-63^\circ\text{C}$ .

**X-ray Diffraction Study.** A rather irregular opaque dark red crystal of approximate size  $0.17 \times 0.27 \times 0.28$  mm was mounted on our Syntex P2<sub>1</sub> diffractometer, and data were collected as described previously.<sup>7</sup> (See Table I.) All data were converted to  $|F_o|$  values following correction for absorption and for Lorentz and polarization factors. Any reflection with  $I(\text{net}) < 0$  was assigned a value of  $|F_o| = 0$ . No data were rejected.

All calculations were performed with the SUNY-Buffalo modified Syntex XTL system on a Data General NOVA 1200 computer. The structure was solved with use of MULTAN<sup>8</sup> and difference-Fourier syntheses. Refinement led smoothly to convergence with  $R_F = 5.7\%$ ,

- (1) For previous papers in the series see: (a) Part 18: Churchill, M. R.; Wasserman, H. J. *Inorg. Chem.* **1981**, *20*, 2905-2909. (b) Part 19: Churchill, M. R.; Hollander, F. J. *Ibid.* **1981**, *20*, 4124-4128. (c) Part 20: Churchill, M. R.; Bueno, C.; Kennedy, S.; Bricker, J. C.; Plotkin, J. S.; Shore, S. G. *Ibid.* **1982**, *21*, 627-633. (d) Part 21: Shapley, J. R.; Samkoff, D. E.; Bueno, C.; Churchill, M. R. *Ibid.* **1982**, *21*, 634-639.
- (2) SUNY at Buffalo.
- (3) The Ohio State University.
- (4) Moss, J. R.; Graham, W. A. G. *J. Organomet. Chem.* **1970**, *23*, C23.
- (5) Geoffroy, G. L.; Gladfelter, W. L. *J. Am. Chem. Soc.* **1977**, *99*, 7565-7573.
- (6) Plotkin, J. S.; Alway, D. G.; Weisenberger, C. R.; Shore, S. G. *J. Am. Chem. Soc.* **1980**, *102*, 6156-6157.

(7) Churchill, M. R.; Lashewycz, R. A.; Rotella, F. J. *Inorg. Chem.* **1977**, *16*, 265-271.

(8) Germain, G.; Main, P.; Woolfson, M. M. *Acta Crystallogr., Sect. A* **1971**, *A27*, 368.

Table II. Atomic Coordinates for  $(\mu\text{-H})_2\text{Os}_3\text{Fe}(\text{CO})_{13}$ 

atom	x	y	z	$B_{\text{iso}}, \text{\AA}^2$
Os(1)	0.17390 (2)	0.27055 (7)	0.09652 (5)	
Os(2)	0.13756 (2)	0.21553 (7)	0.25953 (5)	
Os(3)	0.10245 (2)	0.44006 (7)	0.11062 (5)	
Fe	0.08933 (8)	0.1731 (3)	0.05674 (17)	
O(1)	0.2438 (7)	0.501 (2)	0.1772 (16)	
O(2)	0.1485 (5)	0.3681 (15)	-0.1243 (10)	
O(3)	0.2490 (6)	0.073 (2)	0.0890 (15)	
O(4)	0.0532 (5)	0.1706 (16)	0.3176 (12)	
O(5)	0.1967 (5)	0.3154 (16)	0.4718 (10)	
O(6)	0.1624 (7)	-0.0870 (14)	0.3108 (13)	
O(7)	0.0688 (5)	0.5315 (16)	-0.1143 (10)	
O(8)	0.0321 (6)	0.5995 (17)	0.1662 (12)	
O(9)	0.1675 (6)	0.6844 (15)	0.1725 (13)	
O(10)	0.0462 (8)	-0.067 (2)	0.1078 (14)	
O(11)	0.1488 (5)	-0.0451 (13)	0.0322 (13)	
O(12)	0.0065 (5)	0.2966 (16)	0.0680 (12)	
O(13)	0.0466 (6)	0.1619 (17)	-0.1681 (10)	
C(1)	0.2166 (8)	0.418 (2)	0.1505 (16)	3.6 (4)
C(2)	0.1579 (6)	0.330 (2)	-0.0417 (14)	2.6 (3)
C(3)	0.2209 (8)	0.145 (2)	0.0947 (17)	4.3 (5)
C(4)	0.0848 (7)	0.185 (2)	0.2949 (14)	2.8 (4)
C(5)	0.1752 (7)	0.277 (2)	0.3925 (15)	2.9 (4)
C(6)	0.1537 (7)	0.025 (2)	0.2878 (14)	2.9 (4)
C(7)	0.0818 (7)	0.496 (2)	-0.0274 (14)	2.8 (3)
C(8)	0.0576 (7)	0.542 (2)	0.1449 (14)	2.7 (3)
C(9)	0.1457 (8)	0.588 (2)	0.1506 (16)	3.7 (4)
C(10)	0.0658 (7)	0.027 (2)	0.0898 (15)	3.5 (4)
C(11)	0.1348 (7)	0.061 (2)	0.0501 (15)	3.3 (4)
C(12)	0.0428 (7)	0.279 (2)	0.0702 (14)	2.9 (4)
C(13)	0.0625 (7)	0.173 (2)	-0.0833 (16)	3.1 (4)
H(1)	0.199 (6)	0.220 (16)	0.244 (12)	2.75
H(2)	0.121 (6)	0.397 (17)	0.262 (12)	2.75

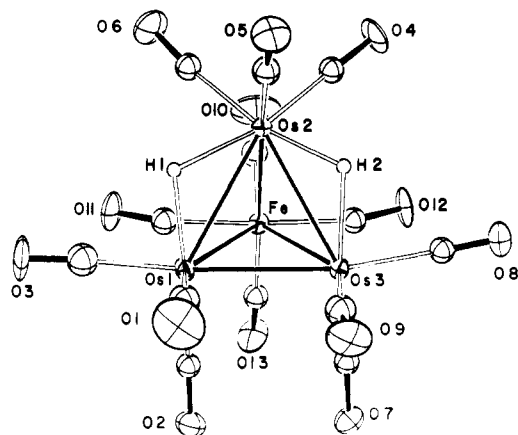


Figure 1. Labeling of atoms in the  $(\mu\text{-H})_2\text{Os}_3\text{Fe}(\text{CO})_{13}$  molecule (ORTEP-II diagram: 30% ellipsoids). Note the approximate  $C_3$  symmetry of the molecule.

$R_wF = 6.2\%$ , and  $\text{GOF} = 1.53^9$  for 212 parameters refined against 2598 reflections [ $R_F = 5.1\%$ ,  $R_wF = 6.2\%$ ,  $\text{GOF} = 1.59$  for those 2339 reflections with  $|F_o| > 3\sigma(|F_o|)$ ]. A final difference-Fourier synthesis was devoid of significant features.

During the calculations the analytical forms for neutral atoms<sup>10a</sup> were corrected for both the  $\Delta f'$  and the  $i\Delta f''$  terms of anomalous dispersion.<sup>10b</sup> The function minimized was  $\sum w(|F_o| - |F_c|)^2$  with  $w = [(\sigma(|F_o|))^2 + (0.030|F_o|)^2]^{-1}$ .

Final positional parameters are collected in Table II. Anisotropic thermal parameters are in Table IIS (supplementary material).

### Description of the Structure

The crystal consists of ordered units of  $(\mu\text{-H})_2\text{Os}_3\text{Fe}(\text{CO})_{13}$  that are mutually separated by normal van der Waals distances.

Table III. Selected Interatomic Distances ( $\text{\AA}$ ) for the  $(\mu\text{-H})_2\text{Os}_3\text{Fe}(\text{CO})_{13}$  Molecule

(A) Metal-Metal Distances			
Os(1)-Os(2)	2.934 (1)	Os(2)-Os(3)	2.937 (1)
Os(1)-Os(3)	2.847 (1)	Os(2)-Fe	2.717 (2)
Os(1)-Fe	2.686 (3)	Os(3)-Fe	2.686 (3)
(B) Metal-Carbonyl Distances			
Os(1)-C(1)	1.922 (22)	Os(1)···O(1)	3.053 (22)
Os(1)-C(2)	1.896 (18)	Os(1)···O(2)	3.039 (13)
Os(1)-C(3)	1.923 (26)	Os(1)···O(3)	3.067 (21)
Os(2)-C(4)	1.914 (22)	Os(2)···O(4)	3.071 (17)
Os(2)-C(5)	1.901 (20)	Os(2)···O(5)	3.034 (14)
Os(2)-C(6)	1.916 (19)	Os(2)···O(6)	3.056 (14)
Os(3)-C(7)	1.876 (19)	Os(3)···O(7)	3.058 (14)
Os(3)-C(8)	1.916 (21)	Os(3)···O(8)	3.018 (19)
Os(3)-C(9)	1.919 (23)	Os(3)···O(9)	3.047 (17)
Fe-C(10)	1.737 (22)	Fe···O(10)	2.916 (20)
Fe-C(13)	1.828 (20)	Fe···O(13)	2.936 (14)
(C) "Semibridging" Carbonyl Distances			
Fe-C(11)	1.823 (22)	Fe-C(12)	1.854 (22)
Os(1)-C(11)	2.341 (20)	Os(3)-C(12)	2.346 (21)
Fe···O(11)	2.925 (16)	Fe···O(12)	2.921 (16)
C(11)-O(11)	1.184 (25)	C(12)-O(12)	1.142 (28)
(D) Metal-Hydride Distances			
Os(1)-H(1)	1.98 (16)	Os(2)-H(2)	1.84 (16)
Os(2)-H(1)	2.01 (20)	Os(3)-H(2)	2.01 (16)
(E) Carbon-Oxygen Distances			
C(1)-O(1)	1.136 (32)	C(7)-O(7)	1.182 (23)
C(2)-O(2)	1.144 (23)	C(8)-O(8)	1.102 (28)
C(3)-O(3)	1.146 (33)	C(9)-O(9)	1.133 (28)
C(4)-O(4)	1.157 (28)	C(10)-O(10)	1.183 (30)
C(5)-O(5)	1.134 (24)	C(13)-O(13)	1.111 (24)
C(6)-O(6)	1.142 (24)		

Figure 1 shows the scheme used for labeling atoms, while Figure 2 provides a stereoscopic view of the molecule. Interatomic distances and their estimated standard deviations (esd's) are collected in Table III, while important interatomic angles are listed in Table IV.

The molecule is based upon a closed tetrahedral  $\text{Os}_3\text{Fe}$  cluster. There are the usual 60 valence electrons associated with a tetrahedral array (three  $d^8$  Os(0) atoms, one  $d^8$  Fe(0) atom, one electron from each hydride ligand, and two electrons from each carbonyl group). Each osmium atom is linked to two terminal carbonyl ligands. The iron atom is bound to two terminal carbonyl ligands and to two "semibridging" carbonyl ligands, the first interacting with Os(1) and the second with Os(3). The structure is completed by two bridging hydride ligands (which were located and refined in the course of the structural analysis) spanning the Os(1)-Os(2) and Os(2)-Os(3) bonds.

The intermetallic distances within the cluster fall into three classes. (Note that the designations "short", "normal", and "long" are used in a local, comparative sense.)

(a) "Normal" Metal-Metal Bond Distances. The Os(1)-Os(3) bond length of 2.847 (1)  $\text{\AA}$  and the Os(2)-Fe bond distance of 2.717 (2)  $\text{\AA}$  are considered to be normal, since there are no bridging ligands present on these tetrahedral edges that might otherwise interfere with the metal-metal bond order. Although the Os(1)-Os(3) bond length of 2.847 (1)  $\text{\AA}$  is 0.03  $\text{\AA}$  shorter than the mean value of 2.877 (3)  $\text{\AA}$  in the triangular species  $\text{Os}_3(\text{CO})_{12}$ ,<sup>11</sup> it is comparable with unbridged osmium-osmium distances in neutral tetrahedral cluster complexes: viz., 2.822 (1)  $\text{\AA}$  in  $(\mu\text{-H})_4\text{Os}_4(\text{CO})_{11}(\text{CNMe})$ ,<sup>12</sup> 2.784 (2)-2.799 (2)  $\text{\AA}$  in  $(\mu\text{-H})\text{Os}_3\text{W}(\text{CO})_{12}(\eta^5\text{-C}_5\text{H}_5)$ ,<sup>13</sup> 2.825

(9)  $R_F = [\sum |F_o| - |F_c|] / \sum |F_o| \times 100$  (%);  $R_wF = [\sum w(|F_o| - |F_c|)^2 / \sum w|F_o|^2]^{1/2} \times 100$  (%);  $\text{GOF} = [\sum w(|F_o| - |F_c|)^2 / (\text{NO} - \text{NV})]^{1/2}$  (NO = number of observations; NV = number of variables).

(10) "International Tables for X-Ray Crystallography"; Kynoch Press: Birmingham, England, 1974; Vol. 4: (a) pp 99-101; (b) pp 149-150.

(11) Part 1: Churchill, M. R.; DeBoer, B. G. *Inorg. Chem.* **1977**, *16*, 878-884.

(12) Part 14: Churchill, M. R.; Hollander, F. J. *Inorg. Chem.* **1980**, *19*, 306-310.

(13) Part 10: Churchill, M. R.; Hollander, F. J. *Inorg. Chem.* **1979**, *18*, 843-848.

**Table IV.** Selected Interatomic Angles (Deg) for  $(\mu\text{-H})_2\text{Os}_3\text{Fe}(\text{CO})_{13}$ 

(A) Intermetallic Angles			
Os(2)-Os(1)-Os(3)	61.04 (2)	Os(1)-Os(3)-Os(2)	60.94 (2)
Os(2)-Os(1)-Fe	57.62 (6)	Os(1)-Os(3)-Fe	57.99 (6)
Os(3)-Os(1)-Fe	58.00 (6)	Os(2)-Os(3)-Fe	57.58 (6)
Os(1)-Os(2)-Os(3)	58.02 (2)	Os(1)-Fe-Os(2)	65.78 (6)
Os(1)-Os(2)-Fe	56.60 (6)	Os(1)-Fe-Os(3)	64.01 (6)
Os(3)-Os(2)-Fe	56.57 (6)	Os(2)-Fe-Os(3)	65.85 (6)
(B) M-M-CO Angles			
Os(2)-Os(1)-C(1)	104.1 (7)	Os(1)-Os(3)-C(7)	95.1 (6)
Os(2)-Os(1)-C(2)	143.7 (6)	Os(1)-Os(3)-C(8)	169.7 (6)
Os(2)-Os(1)-C(3)	114.2 (7)	Os(1)-Os(3)-C(9)	87.6 (7)
Os(3)-Os(1)-C(1)	90.1 (7)	Os(2)-Os(3)-C(7)	147.5 (6)
Os(3)-Os(1)-C(2)	88.1 (6)	Os(2)-Os(3)-C(8)	109.2 (6)
Os(3)-Os(1)-C(3)	175.1 (7)	Os(2)-Os(3)-C(9)	107.6 (7)
Fe-Os(1)-C(1)	147.6 (7)	Fe-Os(3)-C(7)	91.8 (6)
Fe-Os(1)-C(2)	90.8 (6)	Fe-Os(3)-C(8)	120.8 (6)
Fe-Os(1)-C(3)	118.9 (7)	Fe-Os(3)-C(9)	145.6 (7)
Os(1)-Os(2)-C(4)	147.2 (6)	Os(1)-Fe-C(10)	135.8 (7)
Os(1)-Os(2)-C(5)	114.8 (6)	Os(1)-Fe-C(11)	58.9 (7)
Os(1)-Os(2)-C(6)	100.8 (6)	Os(1)-Fe-C(12)	122.8 (6)
Os(3)-Os(2)-C(4)	98.9 (6)	Os(1)-Fe-C(13)	105.3 (7)
Os(3)-Os(2)-C(5)	113.7 (6)	Os(2)-Fe-C(10)	88.8 (7)
Os(3)-Os(2)-C(6)	149.8 (6)	Os(2)-Fe-C(11)	89.3 (7)
Fe-Os(2)-C(4)	91.8 (6)	Os(2)-Fe-C(12)	88.7 (6)
Fe-Os(2)-C(5)	168.9 (6)	Os(2)-Fe-C(13)	169.4 (7)
Fe-Os(2)-C(6)	94.4 (6)	Os(3)-Fe-C(10)	138.6 (7)
		Os(3)-Fe-C(11)	122.9 (7)
		Os(3)-Fe-C(12)	58.9 (6)
		Os(3)-Fe-C(13)	105.5 (7)
(C) Carbon-Metal-Carbon Angles			
C(1)-Os(1)-C(2)	93.8 (9)	C(10)-Fe-C(11)	86.8 (10)
C(1)-Os(1)-C(3)	92.5 (10)	C(10)-Fe-C(12)	90.1 (10)
C(2)-Os(1)-C(3)	95.9 (9)	C(10)-Fe-C(13)	101.8 (10)
C(4)-Os(2)-C(5)	95.2 (8)	C(11)-Fe-C(12)	176.2 (9)
C(4)-Os(2)-C(6)	89.4 (8)	C(11)-Fe-C(13)	90.8 (9)
C(5)-Os(2)-C(6)	94.2 (9)	C(12)-Fe-C(13)	91.9 (9)
C(7)-Os(3)-C(8)	95.3 (8)	C(11)··Os(1)-C(1)	168.0 (8)
C(7)-Os(3)-C(9)	91.7 (9)	C(11)··Os(1)-C(2)	93.4 (8)
C(8)-Os(3)-C(9)	92.9 (9)	C(11)··Os(1)-C(3)	77.1 (9)
		C(12)··Os(3)-C(7)	89.7 (8)
		C(12)··Os(3)-C(8)	78.7 (8)
		C(12)··Os(3)-C(9)	171.6 (8)
(D) Metal-Carbon-Oxygen Angles			
Os(1)-C(1)-O(1)	174.0 (21)	Os(3)-C(7)-O(7)	180.0 (17)
-C(2)-O(2)	178.5 (17)	-C(8)-O(8)	178.9 (18)
-C(3)-O(3)	176.4 (22)	-C(9)-O(9)	173.0 (20)
Os(2)-C(4)-O(4)	178.1 (18)	Fe-C(10)-O(10)	174.2 (20)
-C(5)-O(5)	178.1 (18)	-C(11)-O(11)	152.5 (18)
-C(6)-O(6)	175.1 (18)	-C(12)-O(12)	153.6 (18)
	180.0 (17)	-C(13)-O(13)	174.8 (20)
		Os(1)··C(11)-O(11)	128.1 (16)
		Os(3)··C(12)-O(12)	127.9 (16)
(E) Metal-Metal-Hydride Angles			
Os(3)-Os(1)-H(1)	95.6 (50)	Os(1)-Os(2)-H(2)	91.9 (53)
Fe-Os(1)-H(1)	96.8 (50)	Fe-Os(2)-H(2)	96.0 (53)
Os(3)-Os(2)-H(1)	92.3 (50)	Os(1)-Os(3)-H(2)	91.0 (48)
Fe-Os(2)-H(1)	95.2 (50)	Fe-Os(3)-H(2)	93.0 (48)
(F) Carbon-Metal-Hydride Angles			
H(1)-Os(1)-C(1)	79.6 (50)	H(2)-Os(2)-C(4)	82.0 (53)
-C(2)	172.4 (50)	-C(5)	76.6 (53)
-C(3)	80.8 (50)	-C(6)	166.8 (53)
H(1)-Os(2)-C(4)	168.8 (50)	H(2)-Os(3)-C(7)	173.7 (49)
-C(5)	79.2 (50)	-C(8)	78.7 (49)
-C(6)	81.4 (50)	-C(9)	86.8 (49)
H(1)-Os(1)··C(11)	92.5 (50)	H(2)-Os(3)··C(12)	91.0 (49)
(G) Metal-Hydride-Metal Angles			
Os(1)-H(1)-Os(2)	95 (7)	Os(2)-H(2)-Os(3)	99 (8)
(H) Hydride-Metal-Hydride Angle			
H(1)-Os(2)-H(2)	106 (7)		
(I) Metal-Carbonyl-Metal Angles			
Fe-C(11)··Os(1)	79.3 (8)	Fe-C(12)··Os(3)	78.6 (7)

**Table V.** Comparison of Intermetallic Distances (Å) in  $(\mu\text{-H})_2\text{Os}_3\text{Fe}(\text{CO})_{13}$  and  $(\mu\text{-H})_2\text{Ru}_3\text{Fe}(\text{CO})_{13}$ <sup>a</sup>

bond	Os deriv	Ru deriv <sup>a</sup>	
		molecule 1	molecule 2
M(1)-M(2)	2.934 (1)	2.912 (10)	2.914 (9)
M(2)-M(3)	2.937 (1)	2.885 (8)	2.910 (11)
M(1)-M(3)	2.847 (1)	2.777 (7)	2.816 (8)
M(1)-Fe	2.686 (3)	2.661 (12)	2.654 (9)
M(3)-Fe	2.686 (3)	2.624 (9)	2.619 (9)
M(2)-Fe	2.717 (2)	2.700 (11)	2.700 (9)

<sup>a</sup> See ref 15.

(2)-2.827 (2) Å in  $(\mu\text{-H})_3\text{Os}_3\text{W}(\text{CO})_{11}(\eta^5\text{-C}_5\text{H}_5)$ ,<sup>14</sup> and 2.778 (1) Å in  $(\mu\text{-H})_2\text{Os}_3\text{Co}(\text{CO})_{10}(\eta^5\text{-C}_5\text{H}_5)$ .<sup>1c</sup> The observed osmium-iron distance is close to the ruthenium-iron distance found in  $(\mu\text{-H})_2\text{Ru}_3\text{Fe}(\text{CO})_{13}$ <sup>15</sup> (Ru-Fe = 2.700 (10) Å. (See Table V.) The covalent radius for ruthenium is about 0.01 Å less than that of osmium as is evidenced by the average bond lengths Ru-Ru = 2.854 Å in  $\text{Ru}_3(\text{CO})_{12}$ <sup>16</sup> and Os-Os = 2.877 Å in  $\text{Os}_3(\text{CO})_{12}$ .<sup>11</sup>

(b) "Long" Osmium-Osmium Bond Lengths. The Os(1)-Os(2) and Os(2)-Os(3) distances are equivalent with values of 2.934 (1) Å and 2.937 (1) Å (respectively) and are lengthened appreciably relative to the nonbridged Os(1)-Os(3) distance of 2.847 (1) Å. This is entirely consistent with their being bridged by  $\mu$ -hydride ligands<sup>17</sup> (as shown directly by the diffraction study) and is a result of the Os( $\mu$ -H)Os system being held together by an electron-deficient two-electron, three-center bond. Hydride-bridged Os-Os distances in other *tetranuclear* osmium carbonyl clusters are similarly expanded: 2.941 (2) Å in  $(\mu\text{-H})_3\text{Os}_3\text{W}(\text{CO})_{11}(\eta^5\text{-C}_5\text{H}_5)$ ,<sup>14</sup> 2.932 (2) Å in  $(\mu\text{-H})\text{Os}_3\text{W}(\text{CO})_{12}(\eta^5\text{-C}_5\text{H}_5)$ ,<sup>13</sup> 2.956 (1)-2.971 (1) Å in  $(\mu\text{-H})_4\text{Os}_4(\text{CO})_{11}(\text{CNMe})$ ,<sup>12</sup> 2.893 (1)-2.909 (1) Å in  $(\mu\text{-H})_3\text{Os}_3\text{Co}(\text{CO})_{13}$ ,<sup>18</sup> and 2.870 (1)-2.940 (1) Å in  $(\mu\text{-H})_2\text{Os}_3\text{Co}(\text{CO})_{10}(\eta^5\text{-C}_5\text{H}_5)$ <sup>1c</sup> [the Ru(H)Ru distances are 2.885 (8)-2.914 (9) Å in  $(\mu\text{-H})_2\text{Ru}_3\text{Fe}(\text{CO})_{13}$ ].<sup>15</sup> It is worth noting that the two  $\mu$ -hydride ligands in the last complex,  $(\mu\text{-H})_2\text{Ru}_3\text{Fe}(\text{CO})_{13}$ , again span the homonuclear Ru-Ru vectors rather than the Ru-Fe bonds. The hydride ligands bond to the Os(Ru) atoms because it is these that are electronically deficient in the cluster complex; the osmium atoms have a formal electron count of 17 electrons associated with each of them (vide infra) if one ignores the contribution from the "semibridging" carbonyl ligands and the hydride moieties.

(c) "Short" Osmium-Iron Bond Distances. There are two relatively short Os-Fe vectors in the cluster—these two bonds are equivalent [Os(1)-Fe = 2.686 (3) Å and Os(3)-Fe = 2.686 (3) Å] as might be expected from the  $C_s$  symmetry of the molecule. These distances are contracted by 0.031 Å from the nonbridged Os-Fe bond length of 2.717 (2) Å. This presumably is a result of a "semibridging" carbonyl ligand associated with each of these tetrahedral edges [Fe-C(11) = 1.823 (22) Å, Os(1)··C(11) = 2.341 (20) Å, C(11)-O(11) = 1.184 (25) Å,  $\angle\text{Fe-C(11)-O(11)} = 152.5 (18)^\circ$ ,  $\angle\text{Os(1)··C(11)-O(11)} = 128.1 (16)^\circ$ ; Fe-C(12) = 1.854 (22) Å, Os(3)··C(12) = 2.346 (21) Å, C(12)-O(12) = 1.142 (28),  $\angle\text{Fe-C(12)-O(12)} = 153.6 (18)^\circ$ ,  $\angle\text{Os(3)··C(12)-O(12)} = 127.9 (16)^\circ$ ].

(14) Part 9: Churchill, M. R.; Hollander, F. J. *Inorg. Chem.* **1979**, *18*, 161-166.(15) Gilmore, C. J.; Woodward, P. J. *Chem. Soc. A* **1971**, 3453-3458.(16) Churchill, M. R.; Hollander, F. J.; Hutchinson, J. P. *Inorg. Chem.* **1977**, *16*, 2655-2659.(17) (a) Churchill, M. R.; DeBoer, B. G.; Rotella, F. J. *Inorg. Chem.* **1976**, *15*, 1843-1853. (See, especially, the discussion on pp 1848-1852.) (b) Churchill, M. R. *Adv. Chem. Ser.* **1978**, *No. 167*, 36-60.(18) Bhaduri, S.; Johnson, B. F. G.; Lewis, J.; Raithby, P. R.; Watson, D. J. *J. Chem. Soc., Chem. Commun.* **1978**, 343-344.

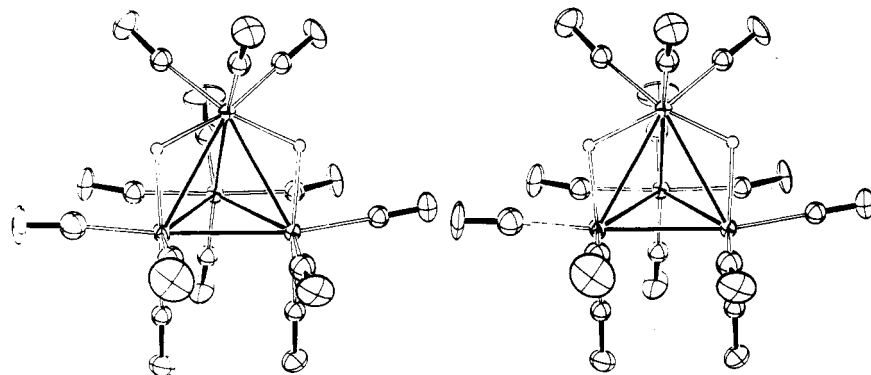


Figure 2. Stereoview of the  $(\mu\text{-H})_2\text{Os}_3\text{Fe}(\text{CO})_{13}$  molecule.

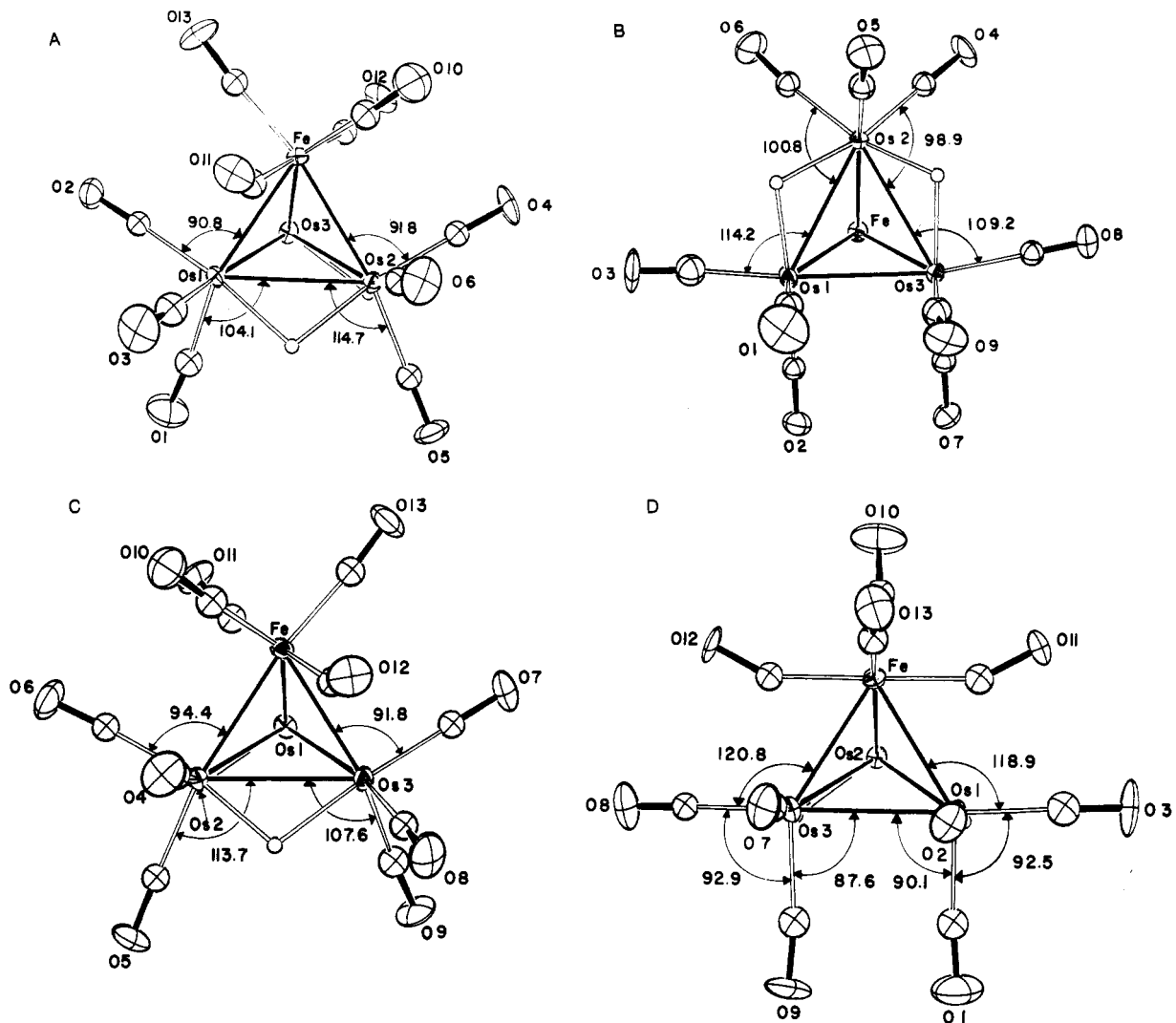


Figure 3. Projections of molecular fragments onto the four triangular faces of the  $\text{Os}_3\text{Fe}$  tetrahedron: (A) the  $\text{Os}(1)\text{-Os}(2)\text{-Fe}$  plane; (B) the  $\text{Os}(1)\text{-Os}(2)\text{-Os}(3)$  plane; (C) the  $\text{Os}(2)\text{-Os}(3)\text{-Fe}$  plane; (D) the  $\text{Os}(1)\text{-Os}(3)\text{-Fe}$  plane (note the bending of the "semibridging"  $\text{Fe-C}(11)\text{-O}(11)$  and  $\text{Fe-C}(12)\text{-O}(12)$  systems; the  $\text{Os}(1)\cdots\text{C}(11)$  and  $\text{Os}(3)\cdots\text{C}(12)$  interactions have been omitted for the sake of clarity).

The  $\mu$ -hydride ligands were located directly from a difference-Fourier synthesis, and their positions were optimized by least-squares refinement. Atom H(1) bridges Os(1) and Os(2) with  $\text{Os}(1)\text{-H}(1) = 1.98$  (16) Å,  $\text{Os}(2)\text{-H}(1) = 2.01$  (20) Å, and  $\angle\text{Os}(1)\text{-H}(1)\text{-Os}(2) = 95$  (7) $^\circ$ ; H(2) bridges Os(2) and Os(3) with  $\text{Os}(2)\text{-H}(2) = 1.85$  (16) Å,  $\text{Os}(3)\text{-H}(2) = 2.02$  (16) Å, and  $\angle\text{Os}(2)\text{-H}(2)\text{-Os}(3) = 99$  (8) $^\circ$ . While the hydride ligands are located with rather poor precision (as expected, with  $Z(\text{H}) = 1$  vs.  $Z(\text{Os}) = 76$ ), one may easily observe their effects on the ligand distribution about the tetrahedral metal cluster.

We have previously commented<sup>1c,14</sup> that bridging hydride ligands in tetrahedral clusters can occur at various angles about the bridged metal-metal vector. Obvious symmetrical possibilities include (a) the case where an  $\text{M}_1\text{-H-M}_2$  plane bisects the exterior angle between the  $\text{M}_1\text{-M}_3\text{-M}_2$  and  $\text{M}_1\text{-M}_4\text{-M}_2$  tetrahedral faces meeting at  $\text{M}_1\text{-M}_2$  (see I) and (b) cases where the  $\text{M}_1\text{-H-M}_2$  plane is coplanar with one of the two triangular faces meeting at the  $\text{M}_1\text{-M}_2$  edge—either with  $\text{M}_1\text{-M}_3\text{-M}_2$  (as in II) or with  $\text{M}_1\text{-M}_4\text{-M}_2$  (as in III). A continuum of less symmetrical locations between or exterior to these positions is, in principle, possible.

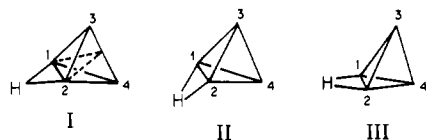


Figure 3 shows portions of the molecule projected, in turn, onto each of the four triangular faces of the tetrahedral cluster. Atom H(1) lies 0.62 Å above (relative to Figure 3A) the Os(1)–Os(2)–Fe plane, whereas it is 0.88 Å above (relative to Figure 3B) the Os(1)–Os(2)–Os(3) plane. The appropriate dihedral angles are  $[\text{Os}(1)\text{--Os}(2)\text{--Fe}]/[\text{Os}(1)\text{--H}(1)\text{--Os}(2)] = 28^\circ$  and  $[\text{Os}(1)\text{--Os}(2)\text{--Os}(3)]/[\text{Os}(1)\text{--H}(1)\text{--Os}(2)] = 41^\circ$ . The expanded equatorial Os–Os–CO angles in Figure 3A  $[\text{Os}(1)\text{--Os}(2)\text{--C}(5) = 114.7(6)^\circ$  and  $\text{Os}(2)\text{--Os}(1)\text{--C}(1) = 104.1(7)^\circ$ ] and Figure 3B  $[\text{Os}(2)\text{--Os}(1)\text{--C}(3) = 114.2(7)^\circ$  and  $\text{Os}(1)\text{--Os}(2)\text{--C}(6) = 100.8(6)^\circ$ ] confirm that H(1) is in an approximately bisecting position between the Os(1)–Os(2)–Fe and Os(1)–Os(2)–Os(3) planes. Furthermore, this correlation is carried over to the second bridging hydride ligand, which is related to the first by the approximate molecular  $C_s$  symmetry.

Atom H(2) lies 0.54 Å above (relative to Figure 3C) the Os(2)–Os(3)–Fe plane whereas it is 0.85 Å above (relative to Figure 3B) the Os(1)–Os(2)–Os(3) plane. The appropriate dihedral angles here are  $[\text{Os}(3)\text{--Os}(2)\text{--Fe}]/[\text{Os}(3)\text{--H}(2)\text{--Os}(2)] = 26^\circ$  and  $[\text{Os}(1)\text{--Os}(2)\text{--Os}(3)]/[\text{Os}(3)\text{--H}(2)\text{--Os}(2)] = 43^\circ$ . The expanded equatorial Os–Os–CO angles in Figure 3C  $[\text{Os}(3)\text{--Os}(2)\text{--C}(5) = 113.7(6)^\circ$  and  $\text{Os}(2)\text{--Os}(3)\text{--C}(9) = 107.6(7)^\circ$ ] and Figure 3B  $[\text{Os}(2)\text{--Os}(3)\text{--C}(8) = 109.2(6)^\circ$  and  $\text{Os}(3)\text{--Os}(2)\text{--C}(4) = 98.9(6)^\circ$ ] argue for H(2) being close to a bisecting position. Regrettably, the errors on the hydride ligand coordinates are too large for us to be more definitive.

Other points of interest include the following:

(1) The molecule possesses almost perfect  $C_s$  symmetry.  
 (2) There are two clear “semibridging” carbonyl interactions, which help to redistribute electronic charge within the molecule. (See Figure 3D). When the hydride ligands are taken into account, the formal electron count for each of the metal atoms is as follows: Os(1) and Os(3) each have a  $d^8$  Os(0) atom, 3 M–M bonds = 3 electrons, 3 carbonyl ligands = 6 electrons, and 1  $\mu$ -hydride ligand =  $1/2$  electron; sum =  $17\frac{1}{2}$  electrons (electron poor). Os(2) has a  $d^8$  Os(0) atom, 3 M–M bonds = 3 electrons, 3 carbonyl ligands = 6 electrons, and 2  $\mu$ -hydride ligands = 1 electron; sum = 18 electrons (electron correct). Fe has a  $d^8$  Fe(0) atom, 3 M–M bonds = 3 electrons, 4 carbonyl groups = 8 electrons, and no  $\mu$ -hydride ligands; sum = 19 electrons (electron rich). The system Fe–[C(11)–O(11)]...Os(1) ( $\alpha = 0.284$ )<sup>19,20</sup> shifts electronic charge from the electron-rich Fe to the electron-poor Os(1) atom. Similarly, the system Fe–[C(12)–O(12)]...Os(3) ( $\alpha = 0.265$ )<sup>19</sup> shifts electronic charge from the electron-rich Fe to the electron-poor Os(3) atom. The overall effect is shift of charge from the Fe to the two electron-poor osmium atoms. The infrared spectrum<sup>21</sup> suggests that a strong “semibridging” interaction is occurring at room temperature in solution.

(3) Although  $(\mu\text{-H})_2\text{Os}_3\text{Fe}(\text{CO})_{13}$  and  $(\mu\text{-H})_2\text{Ru}_3\text{Fe}(\text{CO})_{13}$  are close to isostructural, they are not isomorphous.  $(\mu\text{-H})_2\text{Ru}_3\text{Fe}(\text{CO})_{13}$ <sup>15</sup> crystallizes in space group  $P2_1/a$  with  $Z = 8$ —i.e., there are two chemically equivalent molecules in the crystallographic asymmetric unit. Table V shows the relationship between distances in  $(\mu\text{-H})_2\text{Os}_3\text{Fe}(\text{CO})_{13}$  and distances in  $(\mu\text{-H})_2\text{Ru}_3\text{Fe}(\text{CO})_{13}$ .

(19) The “ $\alpha$  value” for these systems falls near the strong-interaction end of the semibridging regime ( $0.1 < \alpha < 0.6$ ) suggested by Curtis et al.<sup>20</sup>

(20) Curtis, M. D.; Han, K. R.; Butler, W. M. *Inorg. Chem.* **1980**, *19*, 2096–2101.

(21)  $\nu_{\text{CO}}$  (bridging, in  $\text{cm}^{-1}$ ) 1875 w, 1848 m (see Table II of ref 5).

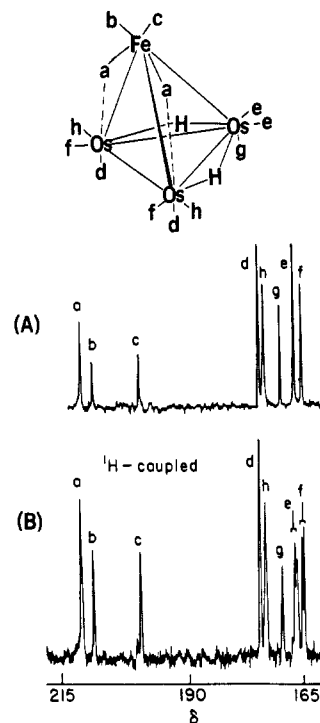


Figure 4. 22.62-MHz  $^{13}\text{C}$  NMR spectra of  $(\mu\text{-H})_2\text{Os}_3\text{Fe}(\text{CO})_{13}$  in  $\text{THF}/\text{CDCl}_3$  at  $-63^\circ\text{C}$ : (A)  $^1\text{H}$  decoupled; (B)  $^1\text{H}$  coupled.

(4) The OC–Os–CO angles for terminal carbonyl ligands are all close to  $90^\circ$ —those within the Os(CO)<sub>3</sub> fragments range from 89.4 (8) to 95.9 (9)°.

(5) There are carbonyl ligands trans to each end of the bridging hydride atoms—appropriate angles are  $\angle\text{H}(1)\text{--Os}(1)\text{--C}(2) = 172.4(50)^\circ$ ,  $\angle\text{H}(1)\text{--Os}(2)\text{--C}(4) = 168.8(49)^\circ$ ,  $\angle\text{H}(2)\text{--Os}(2)\text{--C}(6) = 166.7(53)^\circ$ , and  $\angle\text{H}(2)\text{--Os}(3)\text{--C}(7) = 173.7(49)^\circ$ . If the hydride-bridged metal–metal vectors [Os(1)–Os(2) and Os(2)–Os(3)] are ignored, each osmium atom has a pseudooctahedral geometry (see Figure 3).

(6) Osmium–carbonyl distances are self-consistent and are in the normal range with Os–CO = 1.876 (19)–1.923 (26) Å, Os...O = 3.018 (19)–3.071 (17) Å, and C–O = 1.102 (28)–1.182 (23) Å.

#### NMR Spectra: Discussion

Carbon-13 NMR spectra are consistent with the X-ray structure determination. The limiting  $^{13}\text{C}\{^1\text{H}\}$  spectrum (Figure 4A) indicates that the compound contains eight sets of carbonyl groups with relative intensities of 2:1:1:2:2:1:2:2. These sets are fully consistent with those observed and assigned in the  $^{13}\text{C}$  NMR of the structurally similar compound  $(\mu\text{-H})_2\text{FeRu}_3(\text{CO})_{13}$ .<sup>22</sup> The furthest downfield signal, 213.4 ppm, with relative area 2 is assigned to the semibridging carbonyls, a. Bands consistent with a symmetrical and an asymmetrical stretching frequency in the bridging carbonyl region of the infrared spectrum<sup>5,6,21</sup> are also indicative of two bridging carbonyl groups. The remaining signals in the  $^{13}\text{C}$  NMR spectrum of  $(\mu\text{-H})_2\text{FeOs}_3(\text{CO})_{13}$  are assigned to terminal carbonyl groups.

Carbonyl groups e and f, trans to bridging hydrogens, have signals that are doublets at 166.9 ( $J = 10.3$  Hz) and 165.3 ppm ( $J = 8.8$  Hz) in the proton-coupled spectrum (Figure 4B). Assignment of each of these doublets to a specific carbonyl group e or f cannot be made. Carbonyl groups bound to iron, b and c, cannot be assigned to specific signals, but they probably belong to the signals of areas 1 at 210.8 and 200.6

(22) Geoffroy, G. L.; Gladfelter, W. L. *J. Am. Chem. Soc.* **1977**, *99*, 6775–6778.

ppm since the magnitudes of these shifts are in the range that is normally observed for terminal carbonyls bound to iron in a neutral cluster.<sup>23</sup> Of the three remaining sets of signals, carbonyl g is assigned to the signal of area 1 at 169.9 ppm. Since axial carbonyls in this type of cluster tend to have chemical shifts at lower field than equatorial carbonyls,<sup>23</sup> carbonyls h are assigned to the signal of area 2 at 174.6 ppm and carbonyls d are assigned to the signal of area 2 at 173.4 ppm. Variable-temperature <sup>13</sup>C NMR spectra of ( $\mu$ -H)<sub>2</sub>Os<sub>3</sub>Fe(CO)<sub>13</sub>, recorded from -60° to 70 °C, are consistent

with those reported for ( $\mu$ -H)<sub>2</sub>Ru<sub>3</sub>Fe(CO)<sub>13</sub>.<sup>22</sup> The three distinct fluxional processes suggested for ( $\mu$ -H)<sub>2</sub>Ru<sub>3</sub>Fe(CO)<sub>13</sub><sup>22</sup> are probably also operative in the case of ( $\mu$ -H)<sub>2</sub>Os<sub>3</sub>Fe(CO)<sub>13</sub>.

**Acknowledgment.** This work was supported by the National Science Foundation through Grants CHE80-23448 (M.R.C.) and CHE79-18148 (S.G.S.).

**Registry No.** ( $\mu$ -H)<sub>2</sub>Os<sub>3</sub>Fe(CO)<sub>13</sub>, 12563-74-5; ( $\mu$ -H)<sub>2</sub>Os<sub>3</sub>(CO)<sub>10</sub>, 41766-80-7; Fe<sub>2</sub>(CO)<sub>9</sub>, 15321-51-4.

**Supplementary Material Available:** Listings of anisotropic thermal parameters (Table IIS), least-squares planes, and observed and calculated structure factor amplitudes (29 pages). Ordering information is given on any current masthead page.

(23) Geoffroy, G. L.; Gladfelter, W. L. *Inorg. Chem.* 1980, 19, 2579-2585.

Contribution from the Department of Chemistry,  
University of Vermont, Burlington, Vermont 05405

## Comparison of the Redox Properties of Small Metallacarboranes with Those of Metallocenes and Large Metallacarborane Clusters

WILLIAM E. GEIGER\* and DAVID E. BRENNAN

Received September 25, 1981

Electrochemical data on six iron or cobalt metallacarborane clusters containing 5-7 vertices are presented. Cobalt compounds of the type CpCo(C<sub>2</sub>B<sub>4</sub>H<sub>6</sub>) undergo one oxidation and two reductions, all involving one electron. Only the first reduction, involving Co(II)/Co(I), is completely reversible. The *nido*-cobaltaborane 2-CpCoB<sub>4</sub>H<sub>8</sub> undergoes a reversible reduction to a Co(II) monoanion. 1,2,3-CpFe(C<sub>2</sub>B<sub>4</sub>H<sub>6</sub>), isoelectronic with Cp<sub>2</sub>Fe<sup>+</sup>, is reversibly reduced to formal Fe(II) about 0.8 V negative of the metallocene wave; it also undergoes a one-electron oxidation, although that process is irreversible. Detailed comparison of E° values for metallacarboranes and metallocenes supports the isoelectronic analogy between the two sets of compounds. Compared to their larger metal dicarbollide analogues, the small clusters stabilize high metal oxidation states and destabilize low oxidation states.

Electrochemical studies on metallacarborane clusters have proven to be a valuable probe for the understanding of metal oxidation states in these compounds. Hawthorne and co-workers have reported E° potentials for a large number of metallocarboranes. These and related investigations, which have recently been reviewed,<sup>1</sup> have dealt exclusively with large clusters containing nine or more vertices. In this paper we report the results of an electrochemical investigation of six small metallacarboranes and metallaboranes (1-6; Figure 1) and compare their behavior with that of the electronically similar metallocenes and larger metallacarboranes.<sup>2</sup>

### Electrochemical Methodology and Criteria for Reversibility

Each of the compounds was studied in at least two solvents (usually acetonitrile and dichloromethane) at both mercury and platinum electrodes. This gave a range from about +2.0 to about -2.8 V to search for oxidation or reduction processes. All compounds were investigated by dc polarography, cyclic voltammetry, and, in some cases, phase-selective ac polarography. Polarographic waves were tested for diffusion control by plotting the limiting plateau current against the square root of the mercury column height. Similarly, cyclic voltammetry (CV) measurements always included plots of peak current (i<sub>p</sub>) as a function of the square root of the scan rate. Straight lines showed that each redox process studied was diffusion controlled.

Each wave observed was a one-electron process. This was shown by comparison of the diffusion current constant, I<sub>d</sub><sup>5</sup> with that of the one-electron wave of Cp<sub>2</sub>Co<sup>+0</sup> in the appropriate solvent and by comparison of the CV peak currents with those of Cp<sub>2</sub>Co<sup>+</sup> or Cp<sub>2</sub>Fe at the same scan rate. Plots were made of -E vs. log [i/(i<sub>d</sub> - i)], and slopes of the linear plots were about 60 mV, typical of a reversible one-electron wave. Couples that are simply designated as reversible also displayed ΔE<sub>p</sub> values of no greater than 65 mV at slow CV scan rates (ca. 50 mV/s) and had anodic to cathodic current ratios of about 1 at similar scan rates. Deviations from this behavior are pointed out. A fuller description of the voltammetric measurements is available.<sup>6</sup>

### Cobaltacarboranes

In 1-3, the cobalt atom may be viewed as being in a +3 oxidation state, since the CpCo moiety is bonded to a C<sub>2</sub>B<sub>4</sub>H<sub>6</sub><sup>2-</sup> (or C<sub>2</sub>B<sub>4</sub>H<sub>4</sub>(CH<sub>3</sub>)<sub>2</sub><sup>2-</sup>) ligand. Therefore these compounds are isoelectronic with cobaltocenium ion, Cp<sub>2</sub>Co<sup>+</sup>. This analogy between metallacarboranes and metallocenes was first proposed by Hawthorne<sup>7</sup> and, in at least a qualitative sense, has stood the test of many experimental and theoretical probes over the last 15 years.<sup>8-14</sup> The three cobaltacarboranes are each re-

- (1) Geiger, W. E. In "Metal Interactions with Boron Clusters"; Grimes, R. N., Ed.; Plenum Press: New York, in press.
- (2) Preliminary data on 1 and 2 were previously reported as part of a study ancillary to the investigation of triple-decker sandwich compounds.<sup>3</sup>
- (3) Brennan, D. E.; Geiger, W. E. *J. Am. Chem. Soc.* 1979, 101, 3399.
- (4) All potentials are reported vs. the aqueous saturated calomel electrode.

- (5)  $I = 706nD_0^{1/2} = i_d/Cm^{2/3}t^{1/6}$  (where  $n$  = number of electrons transferred,  $D_0$  = diffusion coefficient of electroactive species,  $C$  = bulk concentration,  $m$  = mercury flow rate,  $t$  = mercury capillary drop time).
- (6) Brennan, D. E. Ph.D. Thesis, University of Vermont, Burlington, VT, 1981.
- (7) Hawthorne, M. F.; Wegner, P. A. *J. Am. Chem. Soc.* 1965, 87, 4392.
- (8) Harris, C. B. *Inorg. Chem.* 1968, 7, 1517.
- (9) Maki, A. H.; Berry, T. E. *J. Am. Chem. Soc.* 1965, 87, 4437.
- (10) Herber, R. H. *Inorg. Chem.* 1969, 8, 174.
- (11) Birchall, R.; Drummond, I. *Inorg. Chem.* 1971, 10, 399.
- (12) Hendrickson, D. N.; Sohn, Y. S.; Gray, H. B. *Inorg. Chem.* 1971, 10, 1559.